Advanced Power Electronic Conversion and Control System for Universal and Flexible Power Management

Stefano Bifaretti, *Member, IEEE*, Pericle Zanchetta, *Member, IEEE*, Alan Watson, *Member, IEEE*, Luca Tarisciotti, and Jon C. Clare, *Senior Member, IEEE*

***Abstract*—The future electricity network has to be able to manage energy coming from different grids as well as from renewable energy sources (RES) and other distributed generation (DG) systems. Advanced power electronic converters can provide the means to control power flow and ensure proper and secure operation of future networks. This paper presents analysis, design, and experimental validation of a back-to-back three-phase ac–dc–ac multilevel converter employed for universal and flexible power management (UNIFLEX-PM) of future electrical grids and its advanced control technique. The proposed system has been successfully tested for bidirectional power flow operation with different grid operating conditions such as voltage unbalance, frequency variation, harmonic distortion, and faults due to short circuits.**

***Index Terms*—Converter control, multilevel converters, power distribution.**

I. Introduction

WITH THE present architecture of the electricity network, most of the electricity is generated in large power stations and transmitted, using a passive transmission line, through high-voltage transmission systems. Power is then delivered to consumers via medium and low-voltage distribution systems [1]. The power flow in this arrangement is only in one direction: from the central power stations to the consumers. Nowadays most of the European countries have started to liberalize the electricity market. In order to enable the electricity market, different distribution system operators (DSOs) will operate on the electricity network transparently and without discrimination under the governance of a regulator [1]. This scenario requires increased penetration of renewable energy sources (RES) and other distributed generation sources (DG) and an active role for DSOs in controlling the network stability, optimizing central and distributed power inputs into the network. Moreover, in order to reach this goal, the architecture of the electricity network should be redesigned on the basis of new paradigms, such as microgrids, an Internet model, and active networks, using the information and communication technologies (ICT) that will transform the existing electrical grid into a smart one [2]. According to [1], active networks, technically and economically, may be the best way to facilitate DG initially in a deregulated market. Their architecture employs an increased number of power input nodes, as a result of DG, bidirectional energy flow is possible and new technologies are emerging that can enable the direct routing of electricity.

New power electronic systems offer ways of controlling the routing of electricity and also provide flexible DG interfaces to the network. Additionally, the power flow control using power electronic converters is needed to ensure stable and secure operation of the grid. Considering such future requirements, this paper presents the application of a power flow control strategy based on a predictive, deadbeat type, current control technique for an advanced back-to-back multilevel power conversion structure used in universal and flexible power management (UNIFLEX-PM). The power conversion structure is outlined first followed by a detailed discussion of the proposed control strategy. A stability analysis is presented and comprehensive simulation are provided for bidirectional power flow operation with different grid operating conditions, in particular on voltage unbalance, frequency variation, harmonic distortion, and faults due to short circuits in the electrical network. Finally, experimental results, obtained on a 300 kVA prototype converter, are presented.

II. Power Converters for High-Voltage Grid Applications

Several topologies, originating from drives applications have been proposed in recent years for medium and high-voltage grid applications. These topologies cover a wide range of applications, e.g., FACTS, STATCOM, DVR, UPFC, IPFC, dc transmission systems, etc., as well as the grid connection of renewable sources [4]–[7]. Most of these applications are based on the traditional two-level voltage source power converter topology [5], [7]. However, due to advances in power semiconductor devices, particularly in the IGBT technology, there has been increasing interest recently in multilevel power converters especially for medium to high-power at high-voltage [8]–[14]. Since the development of the neutral-point clamped three-level converter [15], several alternative multilevel converter topologies

Manuscript received October 09, 2009; revised January 03, 2011; accepted January 29, 2011. Date of publication March 24, 2011; date of current version May 25, 2011. This work was supported by the European Commission under Contract 019794 SES6. Paper no. TSG-00010-2009.

S. Bifaretti is with the Department of Electronic Engineering, University of Rome Tor Vergata, Italy (e-mail: bifaretti@ing.uniroma2.it).

P. Zanchetta, A. Watson, L. Tarisciotti, and J. C. Clare are with the Power Electronics, Machines and Control (PEMC) research group, University of Nottingham, U.K. (e-mail: Pericle.Zanchetta@nottingham.ac.uk; alan.watson@nottingham.ac.uk; Jon.Clare@nottingham.ac.uk).

Color versions of one or more of the figures in this paper are available online at http://ieeexplore.ieee.org.

Digital Object Identifier 10.1109/TSG.2011.2115260

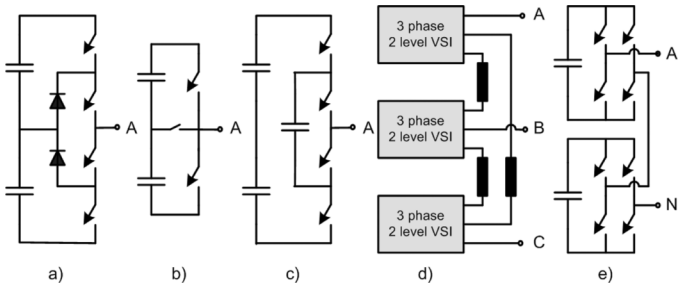

Fig. 1. Multilevel topologies. (a) One leg of a three-level diode clamped converter. (b) One leg of a three-level converter with bidirectional switch interconnection. (c) One leg of a three-level flying capacitor converter. (d) Three-level converter using three two-level converters. (e) One leg of a three-level H-bridge cascaded converter.

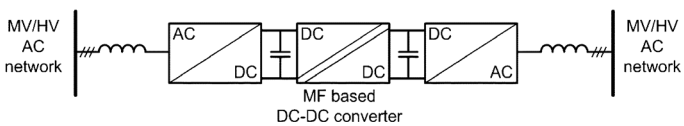

Fig. 2. Generalized multicellular power converter structure.

have been reported in the literature [7]–[16] that can be classified into the following five categories: a) multilevel configurations with diode clamps; b) multilevel configurations with bidirectional switch interconnection; c) multilevel configurations with flying capacitors; d) multilevel configurations with multiple three-phase inverters; and e) multilevel configurations with cascaded single phase H-bridge inverters. Examples of these topologies are shown in Fig. 1.

Among the advantages of these converters, the reduced harmonic content of output voltage and reduced switching losses at the same harmonic performance compared to a two-level converter, are notable.

In order to extend the applicability of the multilevel converters to higher voltage/power applications the interconnection of multilevel structures is proposed in [17]. Three topologies are of interest for these multilevel multicellular converters, namely: the diode-clamped circuit [Fig. 1(a)], the flying capacitor circuit [Fig. 1(c)], and the series isolated H-bridge circuit [Fig. 1(e)]. Among the different topologies, to assure also a modular architecture, a multilevel cascaded single phase H-bridge topology has been selected for the implementation of the UNIFLEX-PM system.

The generalized structure for such a three-phase multicellular converter is shown in Fig. 2.

The topology consists of two ac to dc power conversion stages and a dc to dc conversion stage, based on a medium frequency (MF) transformer, to achieve galvanic isolation between the ac terminals by means of a reduced size system compared to a traditional line frequency transformer.

III. UNIFLEX-PM Structure

The main objective of the UNIFLEX-PM system is to provide a flexible and modular power electronic interface able to connect different kinds of sources and loads including MV electrical networks, RES, and energy storage systems, without requiring large line frequency transformers [3].

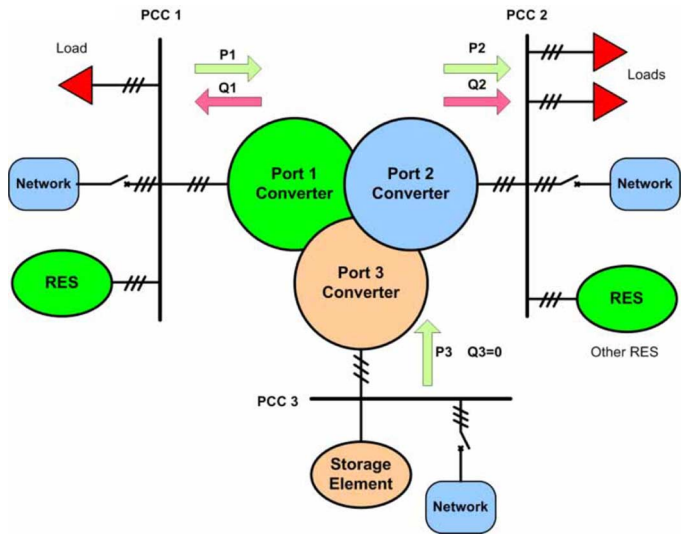

Fig. 3. Block diagram of the UNIFLEX-PM system for grid interaction.

An example functional diagram, shown in Fig. 3, of the UNIFLEX-PM conversion system that is being investigated comprises a three-port power converter, with each port connected to a PCC. Port 1 and Port 2 are used for MV electrical networks, while Port 3 is used mainly to connect the conversion structure to an energy storage system and/or to a low voltage electricity network.

The conversion structure must be able to satisfy the following requirements:

- bidirectional power flow operation at all ports with active and reactive power control capabilities;
- compliance with European and international grid standards for DG connection (see the Appendix for a list of applicable standards) in terms of injected harmonics, robustness to grid voltage distortions, and excursions;
- galvanic isolation between the ports;
- modular architecture providing high reliability and easy maintenance.

Since this latter requirement is a crucial aspect for power electronics systems, both reliability and availability of UNIFLEX-PM are evaluated and compared in [18] against a commercial modular multilevel converter (M^2LC), used in high-voltage direct current (HVDC) applications, and employing line frequency transformers. The comparison has been performed considering the same rated power for both systems and wear-out of the most critical components, such as capacitors, transformers, and power semiconductors. Results have shown that the two systems have similar performances in terms of availability and failures if film capacitors for the dc-link or a redundancy strategy are used in the UNIFLEX-PM [18]. However, it is important to highlight that the UNIFLEX-PM permits important additional functionalities than M^2LC, such as a three-port configuration and voltage asymmetries cancellation (voltage unbalances on one port do not affect the other ports).

Converter control is one of the key elements in achieving the demanding interconnection requirements of DG into MV networks. The basic schematic block of a conversion structure, based on a multistage architecture, that can provide all the above mentioned capabilities, is illustrated in Fig. 4 where only phase

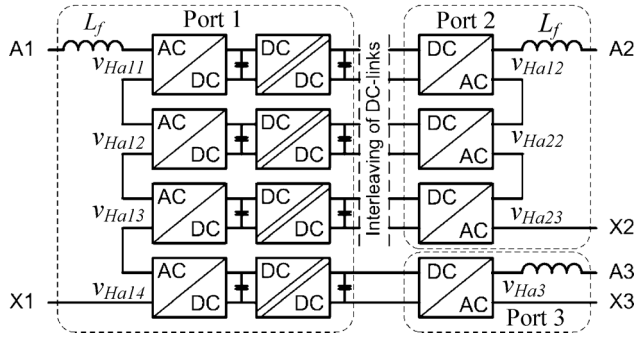

Fig. 4. Structure of one phase of the 3-port UNIFLEX-PM system.

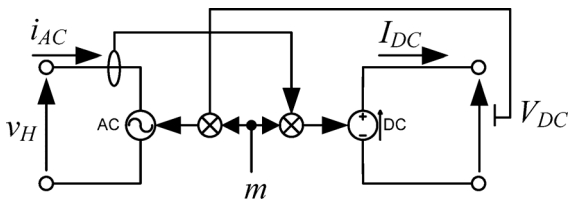

Fig. 5. Average model of an H-bridge converter.

a is represented. A series input filter L_f is included to separate the converter from the grid and provide suitable attenuation of current harmonics.

IV. Simplified Model

In order to test the effectiveness of the implemented control system in a simpler manner, this paper considers a model based on a two-port structure neglecting Port 3.

As a consequence, each phase of Port 1 and Port 2 of the UNIFLEX-PM structure considered employs a conversion structure based on a three-phase 7-level ac-dc cascaded converter. Since each isolated dc/dc conversion stage has a dedicated control which equalizes the voltage on the dc-link at either side of the isolation boundary, an equivalent single dc-link capacitor is used in the model representation.

In order to use the same model for both average simulations, in which only the fundamental component is considered, and switching simulations, which permits to evaluate the effects of converter nonlinear behavior, each H-bridge model is able to support continuous and switching signals.

Each H-bridge is represented by the electrical model shown in Fig. 5 where the relevant variables are defined as follows:

- m is the modulation index used as command input of each H-bridge;
- $i_{\rm ac}$ is the current on the ac side;
- v_H is voltage imposed by H-bridge on the ac side;
- $I_{\rm dc}$ is the current imposed by H-bridge on the dc side;
- $V_{\rm dc}$ is the voltage on the dc-link.

The voltage imposed on the ac side and the current imposed on the dc side depend on the modulation index according to the following relationships:

$$v_H = m \cdot V_{\rm dc}$$
$$I_{\rm dc} = m \cdot i_{\rm ac}.$$

In the switching model, the modulation index m can assume only three discrete values $(-1, 0, 1)$; as a consequence, an H-bridge can impose three different voltage levels $v_H(-V_{\rm dc}, 0, V_{\rm dc})$. On the contrary, if an average behavior is required, m can assume continuous values in range $-1 \div 1$.

Considering a neutral-connected power conversion system, the instantaneous phase to neutral voltage is obtained by summing the dc-link voltages. Referring to Port 1 phase a of the two-port model, the instantaneous voltage v_{Ha1} imposed by the converter on the ac side is achieved using the following relation:

$$v_{Ha1} = \sum_{x=1}^{3} v_{Ha1x} = \sum_{x=1}^{3} V_{\rm dc1x} \cdot m_{a1x} \qquad (1)$$

being v_{Ha1x} the voltage imposed on the ac side by H-bridge x.

V. Control System

Different control systems for grid connected converters, based on natural, stationary or synchronous reference frames, have been proposed in literature [19]–[29]. Synchronous reference frame (dq) control uses the Park transformation to obtain dc values (in steady state) for voltages and currents and makes the control system straightforward to implement. However, the control structure becomes very complex if unbalanced grid voltage conditions have to be accounted for [19]–[22]. Stationary reference frame $(\alpha\beta)$ control uses sinusoidal control variables thus, in order to avoid steady-state errors, PI controllers cannot be used and more complex controllers, such as resonant controllers have to be employed [23], [24]. Finally, a natural reference frame (abc) is normally used with hysteresis [25] or predictive [26]–[28] controllers that give very fast response and are particularly suitable for microprocessor implementation [29]. In this paper a predictive, deadbeat type, current control scheme is proposed for the UNIFLEX-PM conversion structure to control the grid currents and the dc-link voltages. The functional block diagram of the conversion system is shown in Fig. 6, where only Port 1 side is illustrated in detail. However, a similar structure to Port 1 is used for Port 2.

The controller implementation is achieved using four subsystems, as shown in Fig. 6, performing the following tasks at each sampling period T_s:

- PLL block: based on three single-phase phase locked loops (PLLs), provides grid angles for each phase as well as total RMS values for the grid voltages;
- ref. calculation subsystem: computes of the amplitude and phase of the current references $i_{\rm abc}{}^*$ used by predictive block;
- predictive subsystem: performs the current control calculating the instantaneous phase voltages that the converter applies at ac side;
- PWM modulation: determines the switching instants for each power switch of the converter.

A multiloop control structure is selected to regulate the power/dc-link voltage and input line currents at the same time. The outer loop, implemented in the ref. calculation subsystem shown in detail in Fig. 7, regulates active power P and reactive power Q on the basis of active and reactive power references P^* and Q^* imposed by DSO in order to generate the desired power flow. The dc-link voltage reference $V^*_{\rm dca}$ is tracked by adding, to the active power reference value, the output of a PI

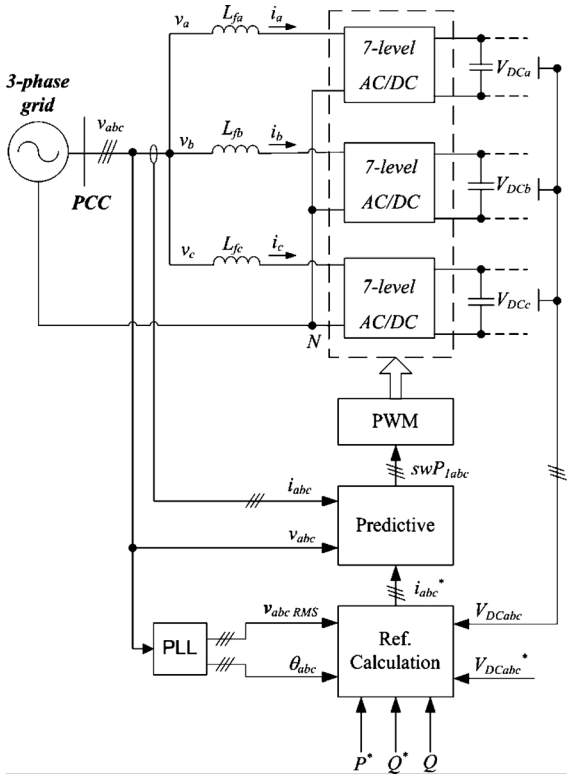

Fig. 6. Functional block diagram of the conversion system.

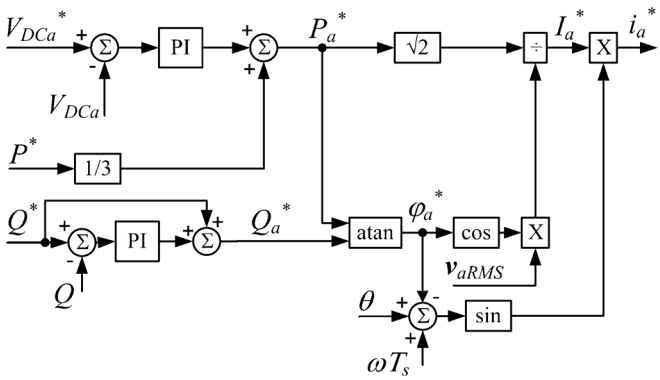

Fig. 7. Detailed structure of ref. calculation subsystem for phase *a* Port 1.

regulator, while the current control action is performed by the predictive algorithm.

Since a neutral-connected conversion system is considered in this paper, the three-phase system acts as three single-phase systems; therefore, the following description of the controller is made referring to phase a Port 1.

Reference current i_a^*, required by the predictive controller at each sampling period, is calculated on the basis of the following sinusoidal function:

$$i_a^* = I_a^* \sin\alpha = I_a^* \sin(\theta + \omega T_s - \varphi_a^*) \tag{2}$$

where the amplitude I_a^* and angle α depend on actual values of active power reference P^*, reactive power reference Q^* and the output the PI regulator used to control the dc-link voltage.

In particular, the amplitude I_a^* is obtained on the basis of the following relationship:

$$I_a^* = \frac{\sqrt{2}P_a^*}{V_{a\mathrm{RMS}} \cdot \cos\varphi_a^*} \tag{3}$$

where

- P_a^* is the active power reference for phase a obtained by weighting the overall active power reference (divided by 3) on the basis of the dc-link error on that phase;
- $V_{a\mathrm{RMS}}$ is the total RMS value of the grid voltage, useful in case of distorted grid voltages;
- φ_a^* is the phase difference between voltage and current at the PCC, needed to produce the desired power factor.

Reference angle φ_a^* is calculated from the following relationship:

$$\varphi_a^* = \mathrm{atan}\frac{Q_a^*}{P_a^*} \tag{4}$$

where Q_a^* is obtained by a feed-forward regulator on the basis of the difference between the desired reactive power Q^* and the measured reactive power Q.

The phase angle α of the reference current i_a^* is calculated by subtracting, from the actual voltage grid angle θ, provided by a PLL, the angle φ_a^*. The term ωT_S is added to account that i_a^* value is calculated at the generic sampling instant k, while the desired output for the converter provided by the controller is applied at next sampling period $k+1$. Since the conversion structure has a neutral connection, the control system uses three separate PLLs, based on the prediction-correction filter proposed in [30] and properly modified for single-phase systems. This method is easy to implement on DSPs, has very good dynamic performance, and considerable robustness against grid frequency variations and harmonic distortions.

The basic equation of the predictive controller model is obtained starting from the following state equation for the inductor L_f:

$$i_j(t+t_0) = i_j(t_0) + \frac{1}{L_f}\int_{t_0}^{t}(v_j - v_{hj})dt \tag{5}$$

where j represents the phase a, b or c. Applying a time discretization to (5) with a sampling period T_s and supposing v_{hj} constant during T_s, the following expression for the voltage v_{hj} is obtained:

$$v_{hj_k} = \frac{L_f}{T_s}(i_{j_k} - i_{j_{k+1}}) + \frac{1}{T_s}\int_{t_k}^{t_k+T_s} v_j dt. \tag{6}$$

In order to impose a zero current error, the control law assumes, at each sampling period, i_{jk+1} equal to the reference current i_{jk}^*; therefore, (6) becomes

$$v_{hj_k} = \frac{L_f}{T_s}(i_{j_k} - i_{j_k}^*) + \frac{1}{T_s}\int_{t_k}^{t_k+T_s} v_j dt. \tag{7}$$

Equation (7) is implemented in the predictive block shown in Fig. 6 and provides the reference voltage value that the converter needs to impose on the ac side to obtain the desired current. To reduce the effects of the harmonics in the grid voltages, the

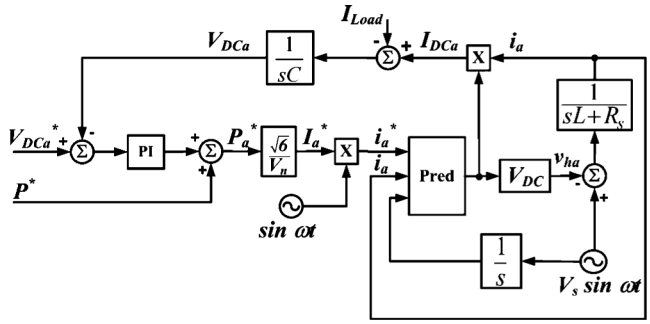

Fig. 8. Block diagram used for stability analysis.

integral of v_j is calculated using the method proposed in [27]. Finally, the PWM modulator implemented in [31] is used to produce the necessary switching signals to generate the desired modulated voltage on the ac side of the converter.

For Port 2, the controller is similar to that of Port 1 except for the active power regulation. In fact, both the active and reactive powers are controlled through PI controllers without any interaction of dc-link voltage. Then, the calculation of the amplitude and phase of the current references, necessary for predictive controller, is the same.

The proposed control system assures fast current control, even with unbalanced and distorted grid conditions, without requiring resonant regulators which can present critical issues on parameter tuning and stability. Moreover, the currents are individually controlled on each phase, adding more flexibility to the UNIFLEX-PM system. This feature enables the UNIFLEX-PM converter to handle all kinds of asymmetries in the grid, e.g., unbalanced voltages such as those caused by asymmetrical faults. Moreover, individual control of currents in each phase can provide advanced grid support functions such as reactive current injection into the faulted phases of an asymmetric fault.

VI. Sensitivity and Stability Analysis

A stability analysis of the systems, including the converter sensitivity to the grid supply inductance (L_s) variation, has been performed, at first, on an approximated linearized model of the UNIFLEX-PM, accounting only for active power control, as shown in the block diagram illustrated in Fig. 8.

This analysis is very important in distribution networks, above all when, given the presence of different microgrids and renewable energy sources, the grid impedance can largely vary according to the network conditions affecting the system control behavior. The linearization procedure has been carried out around the rated operative equilibrium point. Fluctuations of the position of system poles and zero can be therefore recorded as a function of specified parameters variations. The system parameters accounted for the stability analysis are listed in Table I.

The stability of the system has been studied in order to highlight the robustness of the control system to power supply inductance L_s variations. To make the analysis independent from the considered parameters values, the ratio between the power supply inductance L_s and the filter inductance value L_f, used in (7) by the predictive controller, is employed.

TABLE I
UNIFLEX-PM Rated Parameters

Parameters		Units	Value
Rated voltage (line-to-line)	V_n	[kV]	3.3
Rated apparent power / converter	S_{nc}	[kVA]	300
Power Supply inductance	L_s	[mH]	1.7
Input filter inductance	L_f	[mH]	16
Rated output current / H-bridge	I_{nm}	[A]	52.63
DC-link voltage / H-bridge	V_{DC}	[V]	1100
DC-link capacitor / H-bridge	C	[mF]	6.2
Sampling frequency for control	f_s	[kHz]	5

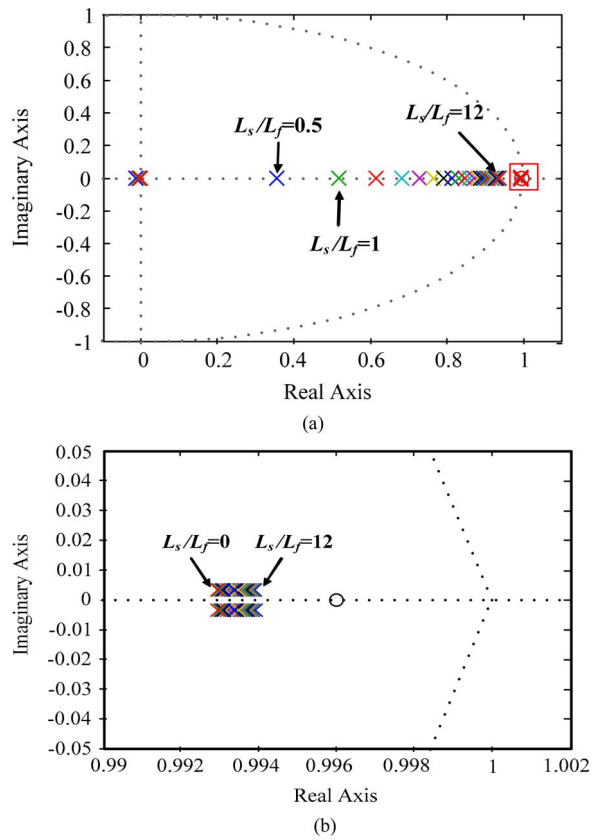

Fig. 9. (a) Pole-zero map of the system. (b) Zoom of the square in (a).

Fig. 9(a) shows the pole/zero map of the current control plant as function of the ratio L_s/L_f. Fig. 9(b) shows the pole zero map of the voltage/active power control loop presenting a slower dynamics [zoom of the red square in Fig. 9(a)]. This analysis indicates that the poles remain inside the unity circle even if the ratio L_s/L_f assumes quite large and impractical values, i.e., the grid becomes very weak.

In order to also verify the sensitivity of the control system performance to L_s/L_f deviations, dc-link voltage variation, gain, and phase shift of the current control loop have been evaluated, as shown respectively in Figs. 10, 11(a), and (b).

From these figures it can be observed that if the ratio L_s/L_f is lower than 4, which is already an improbable value, the system performance is still acceptable.

The control system stability and performance have also been tested against variations of the supply resistance and dc

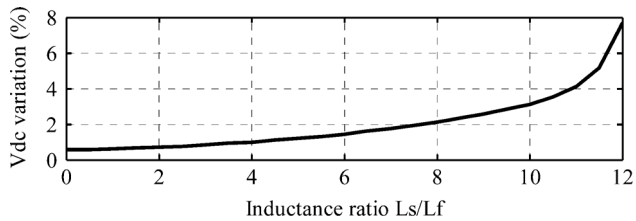

Fig. 10. DC-link voltage variation vs. L_s/L_f.

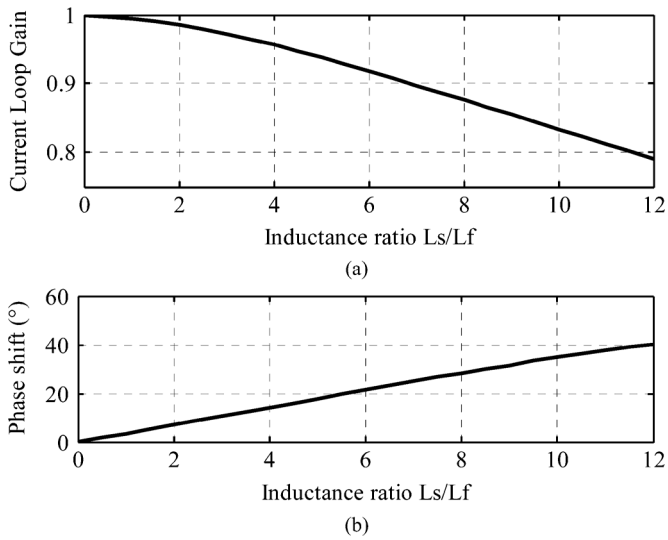

Fig. 11. (a) Current loop gain and (b) phase shift variation versus L_s/L_f.

TABLE II
STEADY-STATE VALUES (IN PU) FOR DIFFERENT OPERATING POINTS

P^*	Q^*	P_{avg}	Q_{avg}	V_{DC_err}	i_{a_err}
0	0.5	0.007	0.489	0.0038	0.044
0	1	0.002	0.993	0.0043	0.055
0.1	0	0.106	0.012	0.0078	0.040
0.3	0	0.305	0.012	0.0066	0.083
0.5	0	0.504	0.013	0.0050	0.089
0.8	0	0.800	0.012	0.0039	0.094
1.0	0	1.006	0.025	0.0023	0.121

voltage fluctuations, showing a very low sensitivity also to these parameters.

In order to evaluate the system stability in operating conditions as close as possible to those of a real implementation, the nonlinear switching model of the converter and the complete control system has been considered. The evaluation has been performed by simulation for different operating points using a switching model of the converter driven with the PWM modulation proposed in [31] specifically developed for UNIFLEX-PM in order to evenly distribute commutation stress on the semiconductors. Results of this evaluation are shown in Table II, which lists, in correspondence of different demands of active (P^*) and reactive power (Q^*), the mean value of active power (P_{avg}), the mean value of reactive power (Q_{avg}), the RMS values of the error of phase a dc-link voltage (V_{dc_err}), the RMS values of the error of phase a line current (i_{a_err}). The results show that the RMS values of the errors on the state variable are limited in all the considered operating points.

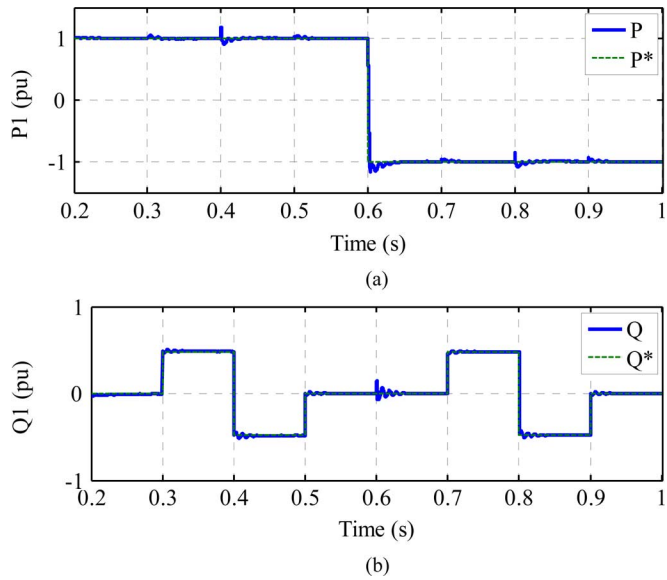

Fig. 12. Simulation results for power flow study in Port 1. (a) Active power. (b) Reactive power.

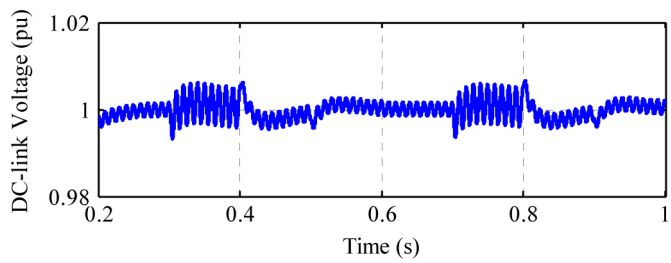

Fig. 13. DC-link voltage on phase *a* Port 1.

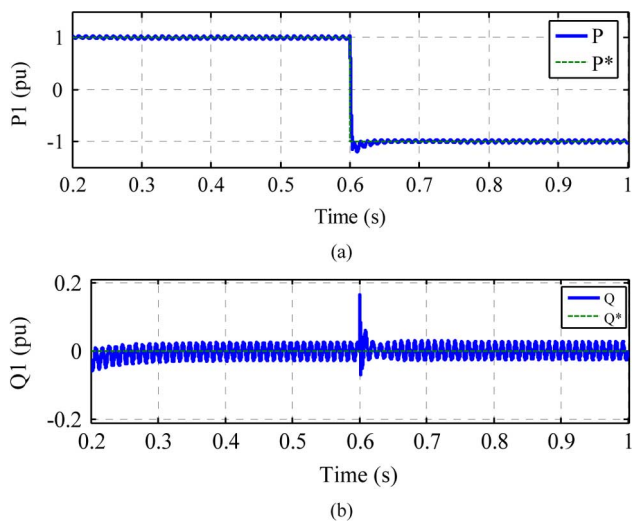

Fig. 14. Power flow under voltage unbalances in Port 1. (a) Active power. (b) Reactive power.

VII. SIMULATION RESULTS

The proposed control strategy has been evaluated under different power flow profiles, grid conditions, and situations such as voltage unbalances, frequency excursions, and harmonic distortion.

Simulation results have been obtained for 5 different study cases, using a complete Matlab-Simulink model of the UNIFLEX-PM system with the parameters listed in Table I and

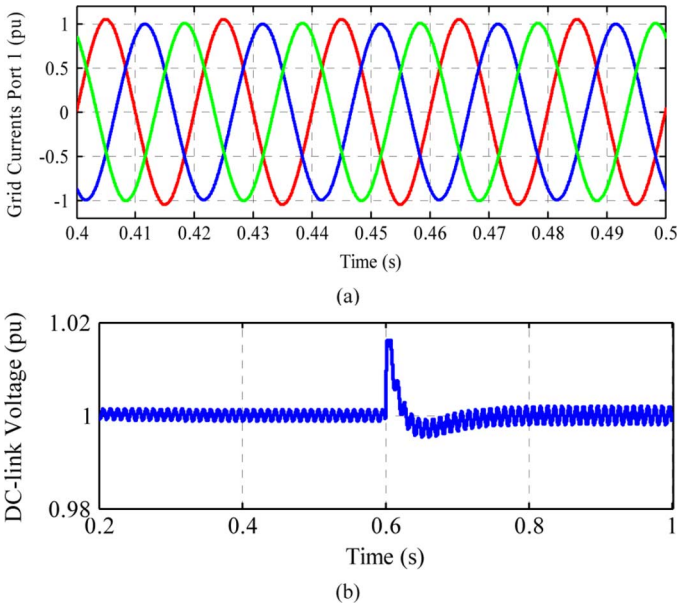

Fig. 15. Simulation results for voltage unbalances in Port 1. (a) Input currents Port 1. (b) DC-link voltage phase *b* Port 1.

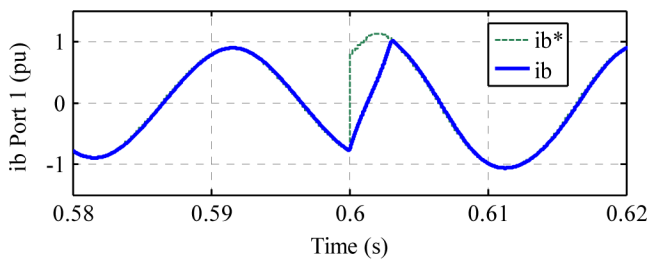

Fig. 16. Phase *b* current tracking during active power step.

taking the power circuits, modulation, and control into account. A bidirectional power flow is simulated using an average model of the UNIFLEX-PM system for the cases A, B, and C; in case D a switching model of the converter, driven with a dedicated PWM modulation [31], has been used whilst in case E the simulation also incorporates harmonics on the grid voltages.

A. Power Flow

A first set of tests have been performed to evaluate the effectiveness of the UNIFLEX-PM system in power flow control using reference step changes both for active and reactive power. The waveforms of active and reactive power (continuous line), shown respectively in Fig. 12(a) and (b), tracks the reference (dashed line) with satisfying dynamics and steady state error. Moreover, Fig. 13 shows, for example, the voltage on the capacitor of phase *b* Port 1 demonstrating that the dc-link voltage is well regulated and presents insignificant error.

B. Voltage Unbalances

Further tests are carried out when the system is delivering 100% of active power and a 3% of voltages unbalance, defined as the ratio between the voltage negative and positive sequences, is applied in the grid at Port 1. Fig. 14(a) and (b) show simulation results for active and reactive power flow control, while Fig. 15(a) and (b) show the grid currents and the dc-link voltage

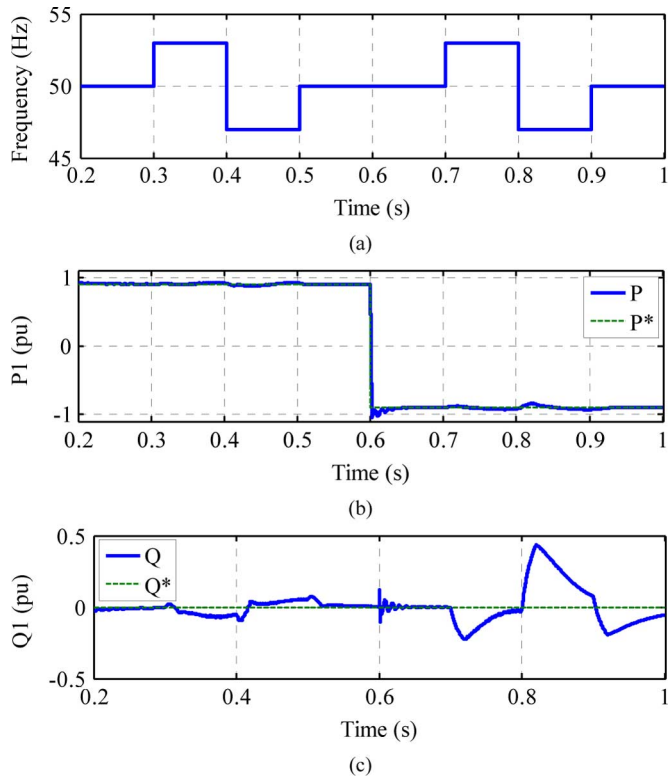

Fig. 17. Power flow under frequency excursions in Port 1. (a) Frequency profile. (b) Active power. (c) Reactive power.

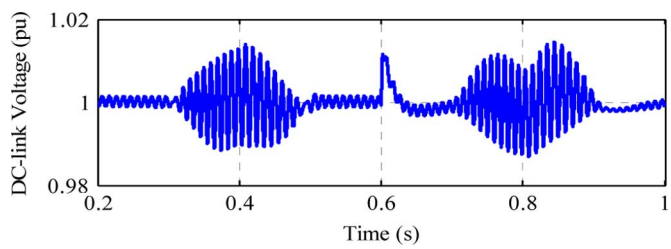

Fig. 18. Simulation results for frequency in Port 1: dc-link voltage.

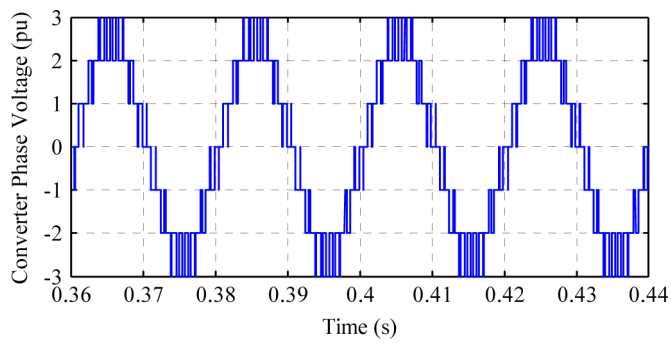

Fig. 19. Modulated voltage produced by the converter.

on phase *b*. It is to be noted that the grid currents are essentially sinusoidal and the active power is well regulated.

The effect of the unbalance causes ripples on the reactive power which cannot be eliminated. Moreover, the dc-link voltage presents a maximum variation of about 1.5% from the nominal value. The effectiveness of predictive current controller can be observed by phase *b* current tracking, illustrated in Fig. 16, when the step variation in the active power shown in Fig. 14(a) is applied at $t = 0.6$ s. The current transient duration,

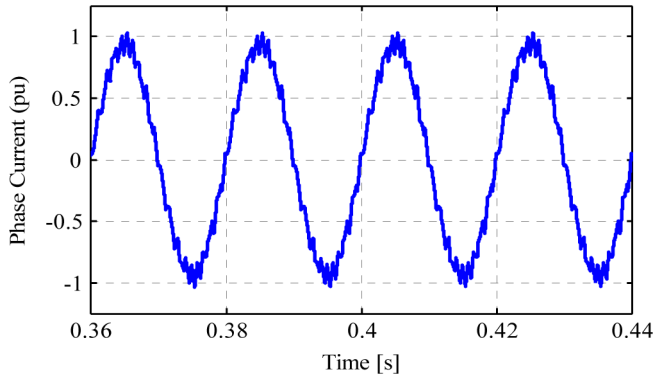

Fig. 20. Phase current produced applying modulated voltage.

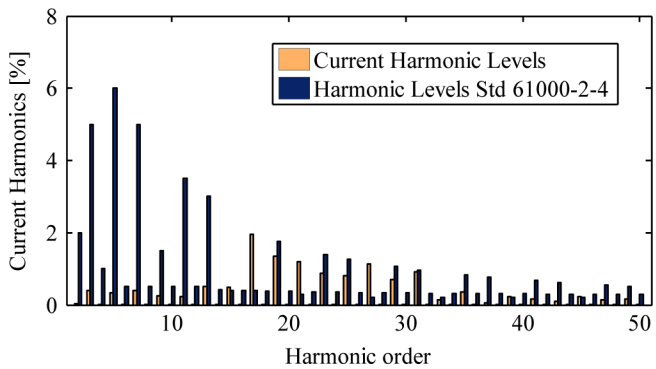

Fig. 21. Harmonic content of phase *a* current.

due to the active power step change, is limited to about 1/5 period; before and after that interval the predictive controller is able to track very accurately the reference current.

C. Frequency Excursions

The behavior of the control systems has been also evaluated when a ±6% frequency variation, with the profile shown in Fig. 17(a), of the grid voltages is applied.

Fig. 17(b) and (c) show the simulation results obtained for active and reactive power flow, while Fig. 18 illustrates the dc-link voltage on phase b which proves, also in this case, to be very well regulated.

D. Harmonic Content

Harmonic study tests were performed to evaluate the current harmonics injected into the grid by the converter modulation. The analysis considers that the power modules deliver 100% active power into the PCC while the reactive power is set to zero. An 1800 Hz switching frequency has been selected for the power converter PWM modulation and the grid voltages have been considered undistorted.

Figs. 19 and 20 show, respectively, the converter output voltage on phase a of Port1 and the corresponding phase current in the above-mentioned operating conditions.

Fig. 21 shows individual harmonics values for the phase current up to the 50th harmonic versus EN 61000-2-4 standard harmonic levels, represented in the figure respectively in the left-side bars and the right-side bars.

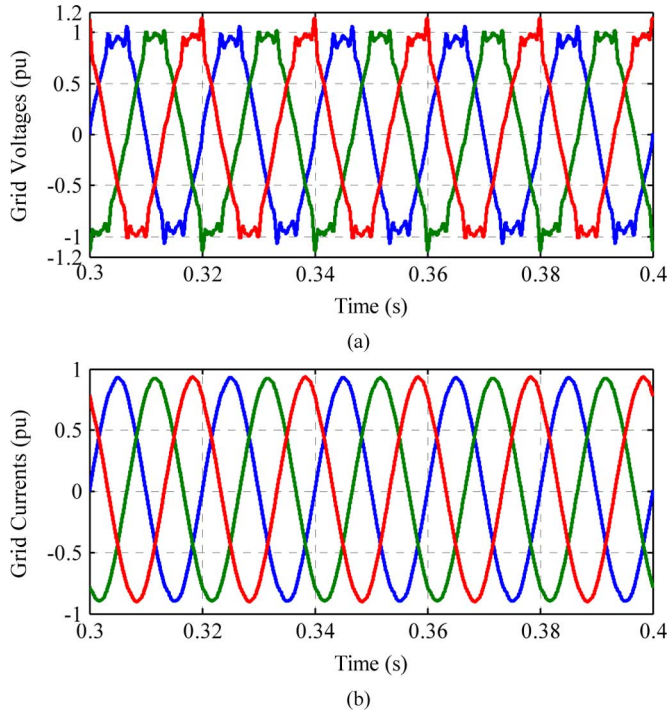

Fig. 22. Effects of distorted grid voltages in Port 1. (a) Grid voltages. (b) Grid currents.

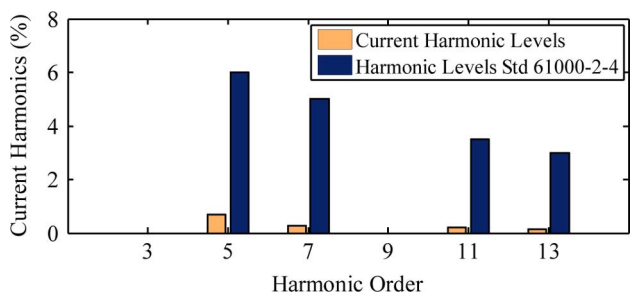

Fig. 23. Effects of distorted grid voltages in Port 1: current harmonics.

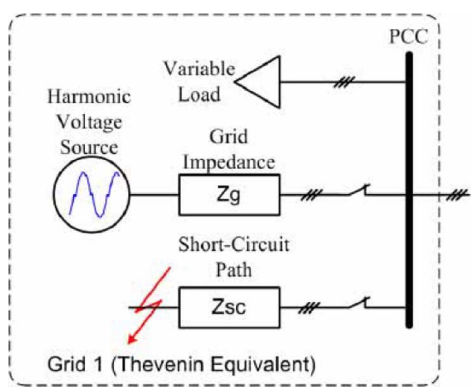

Fig. 24. Structure of the grid model.

The current harmonic levels that exceed the standard values are positioned at harmonic orders 17th, 21th, and 27th; such behavior is due to the intrinsic characteristic of the modulation which evenly distributes the commutations amongst the cascaded cells of the converter, as shown in [31]. A relevant quantity of 3rd harmonic, equal to about 0.5% of the fundamental, is present due to the neutral connection required by this control

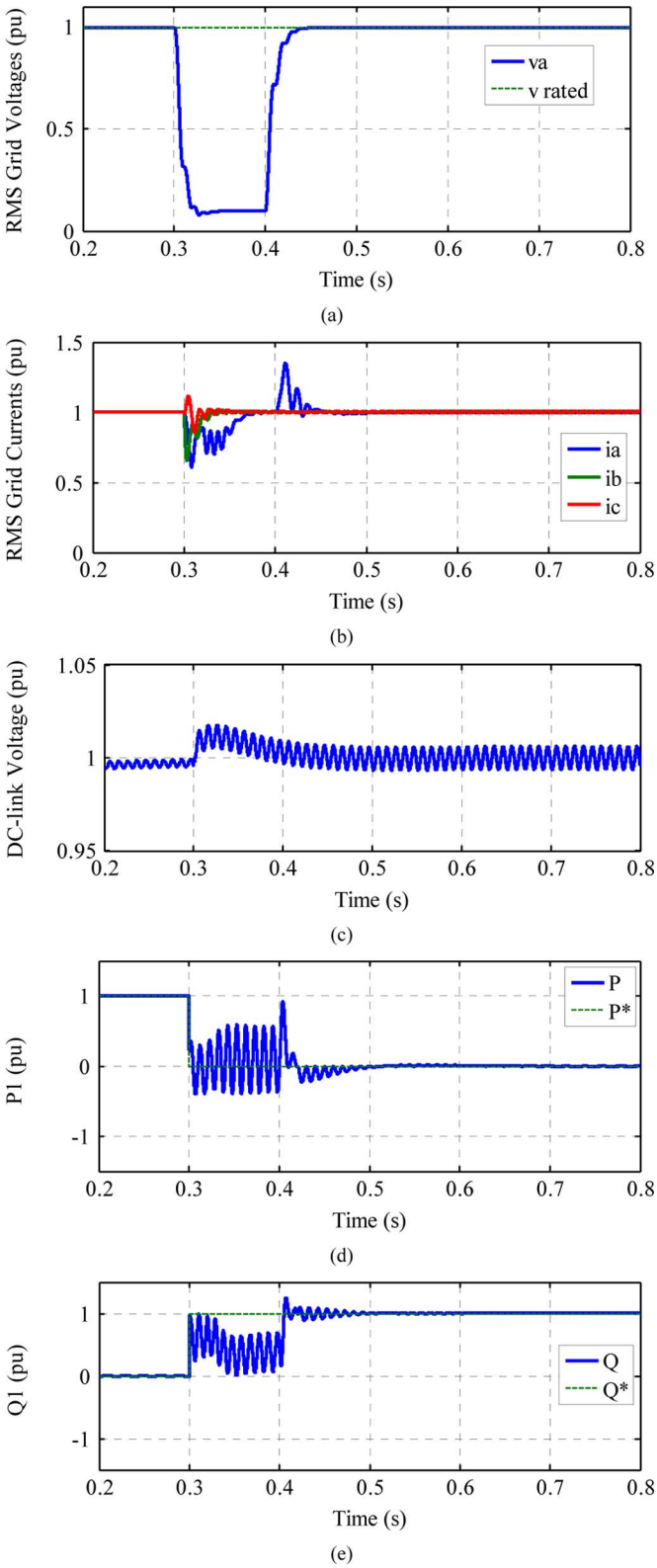

Fig. 25. Simulation results during one-phase short circuit. (a) RMS grid voltages. (b) RMS grid currents. (c) DC-link voltage on phase b. (d) Active power. (e) Reactive power.

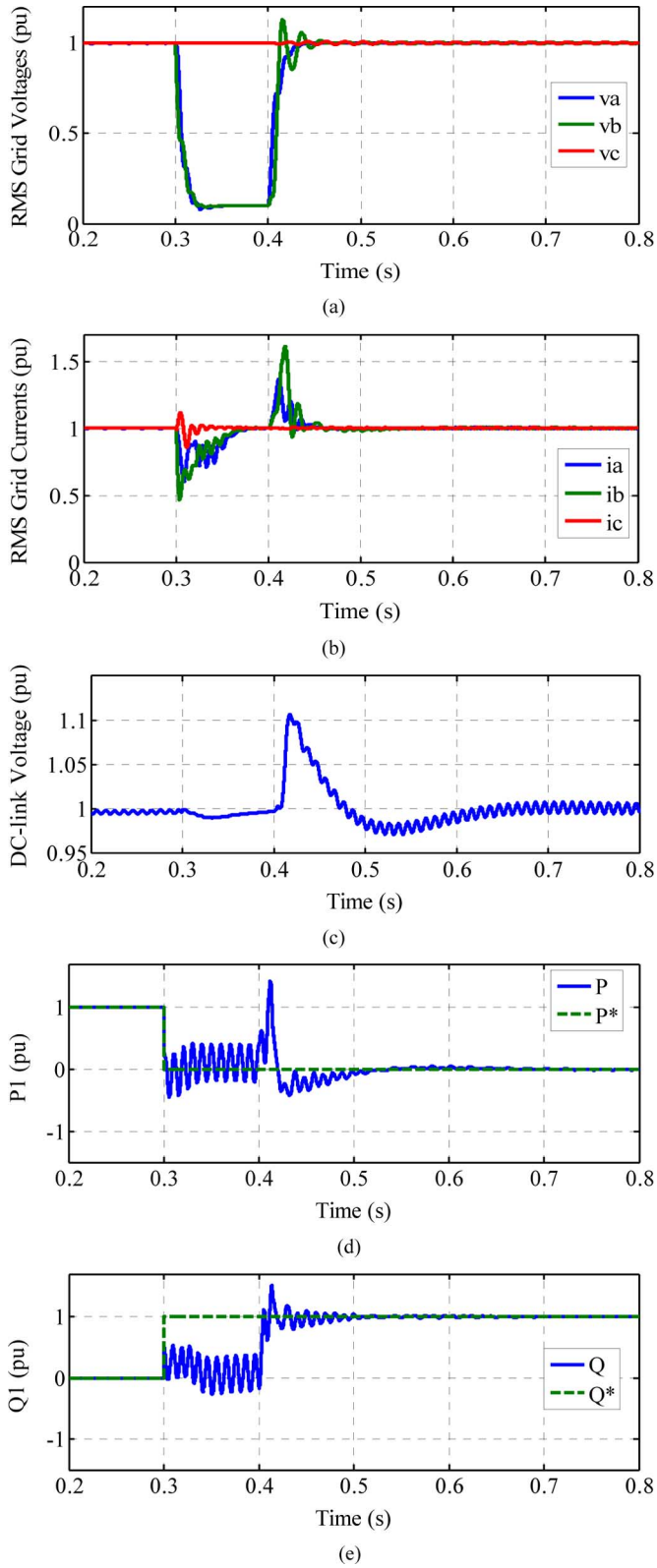

Fig. 26. Simulation results during two-phase with ground short circuit. (a) RMS grid voltages. (b) RMS grid currents. (c) DC-link voltage on phase b. (d) Active power. (e) Reactive power.

strategy; however, this value is much less than the 5% limit imposed by the standard EN 61000-2-4.

Finally, the analysis shows a current THD value of 6.7%, which is significantly lower than 8% limit required by the same standard.

Fig. 27. 300 kVA UNIFLEX-PM prototype.

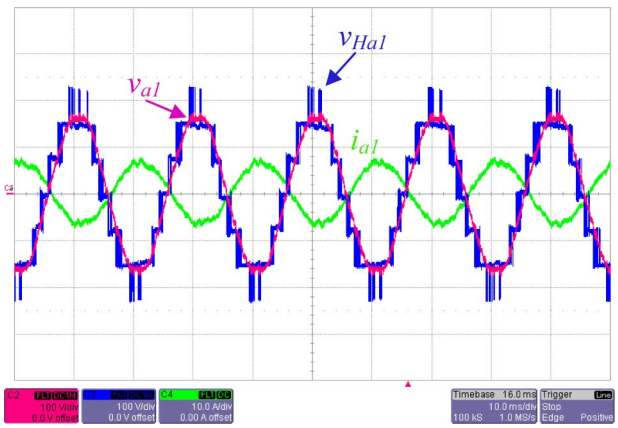

Fig. 28. Experimental results on phase a Port 1: supply voltage (v_{a1}), converter voltage (v_{Ha1}), and phase current (i_{a1}).

E. Effects of Distorted Grid

Another interesting aspect is the performance evaluation of the converter control when the grid voltages are distorted.

In this case, the analysis considers that the power modules deliver 90% active power into the PCC while the reactive power is set to zero. The grid voltages are polluted with 5th, 7th, 11th, and 13th harmonics according to the amplitudes indicated by the standard EN 61000-2-4.

Fig. 22(a) and (b) show, respectively, the waveforms of the grid voltages and the grid currents in Port 1, while in Fig. 23 are indicated individual harmonics values for the phase current (left-side bars) and EN 61000-2-4 harmonics levels (right-side bars). It can be noticed that the proposed control produces almost sinusoidal currents even if the supply voltages are strongly distorted.

F. Faults

The system was simulated also under different faulty operating conditions of the power grid. To this aim a grid model based on Thevenin equivalent with short-circuits capabilities is used as specified in [32] and [33]. A complete structure of this model is shown in Fig. 24.

In this paper one-phase and two-phase with ground short circuits are considered. It is supposed that the fault occurs at the Port 1 and has a duration of 100 ms. Before the event, the power converter is operating at 100% active power and 0% reactive

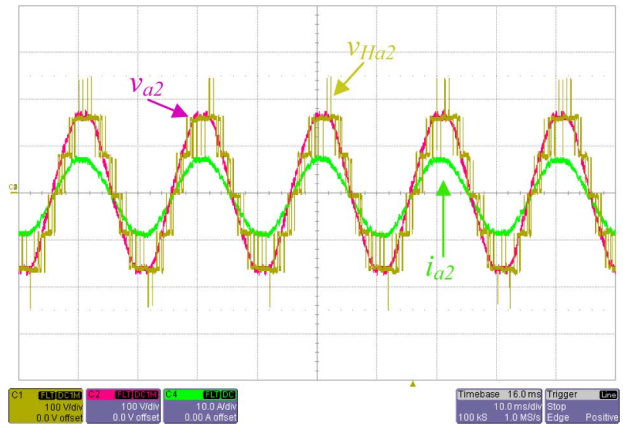

Fig. 29. Experimental results on phase a Port 2: supply voltage (v_{a2}), converter voltage (v_{Ha2}), and phase current (i_{a2}).

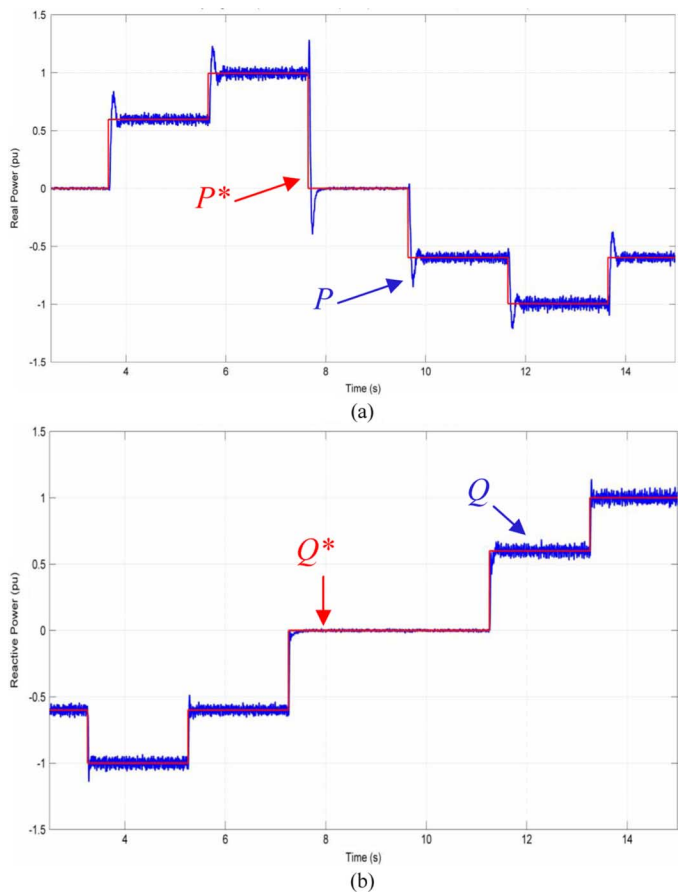

Fig. 30. (a) Active and (b) reactive power flow: active power demand (P^*) and measure (P), reactive power demand (Q^*) and measure (Q).

power. During and after the fault the active power reference is set to zero, while the power converter is delivering 100% reactive current. The short circuit resistance of the grid is selected so that the grid voltage reaches 10% of its rated value.

1) One-Phase Short-Circuit: Fig. 25 shows the system behavior when one-phase short circuit occurs. The input current transient peak is higher than 40% of the rated value [Fig. 25(b)], whilst the dc-link voltage is maintained almost constant [Fig. 25(c)]. After the fault, the control system recovers active and reactive power reference tracking in about 100 ms.

TABLE III
EUROPEAN AND INTERNATIONAL GRID STANDARDS FOR DG CONNECTION

Standard	Year	Title	Topics	Voltage
EN 50160	2000	Voltage characteristics of electricity supplied by public distribution networks	Power quality	LV&MV
EN 50330-1	1999	Photovoltaic semiconductor converters. Part1: Utility interactive fail save protective interface for PV-line commutated converters – Design qualification and type approval.	Principles and test procedure to a failsafe protective interface	LV
IEEE Std 929	2000	IEEE Recommended practice for utility interface of photovoltaic systems	Power quality Voltage disturbances Frequency disturbances Island/non island operation	LV
IEC 61727 CDV	2002	Characteristics of the utility interface for Photovoltaic systems	Power quality Voltage/ frequency disturbances Islanding protection	LV
IEEE Std 1250	1995	IEEE Guide for service to equipment sensitive to momentary voltage disturbances	Power quality Voltage harmonics, flickers Current harmonics Ride-through	any
IEEE Std 1547	2003	IEEE Standard for interconnecting distributed resources with Electric power systems	Power quality Current harmonics Voltage harmonics	any
IEEE Std 519	1992	IEEE Recommended Practices and Requirements for Harmonic Control in Electrical Power Systems	Power quality	any

2) Two-Phase With Ground: Fig. 26 illustrates the simulation results in the case when a two-phase with ground short circuit occurs. The input current transient peak becomes slightly higher than 50% of the rated value and the dc-link voltage transient peak overcomes of 10% the rated dc value. The proposed control is able to recover after active and reactive power transients again in about 100 ms.

VIII. EXPERIMENTAL SETUP AND RESULTS

The 300 kVA prototype converter, assembled and tested at the University of Nottingham, is shown in Fig. 27. The converter is composed of 12 UNIFLEX-PM modules, each comprising 4 H-bridges and a medium frequency transformer. The dc-link capacitance on each side of the converter cell comprises six 4.7 mF capacitors, rated at 450 V. These are connected three in series, two in parallel to produce a dc-link capacitance of approximately 3.2 mF and a voltage rating of 1350 V. The control scheme for the converter is implemented on a Texas Instruments 6713 DSP interfaced to five FPGA cards designed at the University of Nottingham. Control of the dc/dc isolation modules, comprising two H-bridges and the MF transformer, is implemented entirely using the FPGA hardware to relax the computational burden on the DSP. Tracking of the dc-link voltages on each side of the isolation boundary is ensured by the dc/dc converter control loops which act to drive the difference between the dc-link voltages on each side to zero.

Preliminary experimental tests of the proposed conversion system and control technique have been performed, at low voltage, on the UNIFLEX-PM prototype using a two-port configuration and accounting the following parameters: 80 V for dc-link voltage reference, 1.8 kHz control and switching frequency, 115 V_{RMS} for supply voltage on each port.

Fig. 28 shows the multilevel phase a voltage waveform imposed by the converter, the supply voltage, and the corresponding phase current. Fig. 29 shows the same quantities but on phase a of Port 2. Fig. 30 experimentally demonstrates the capabilities of the UNIFLEX-PM converter to effectively control active and reactive power flow.

IX. CONCLUSION

This paper proposes a novel back-to-back three-phase ac–dc–ac 7-level converter structure suitable for universal and flexible power management (UNIFLEX-PM) in the future electricity network and its advanced control system based on a predictive, deadbeat type, solution. The main goal of the system is to provide a flexible and modular power electronic interface able to connect different kinds of sources and loads including MV electrical networks, RES, and energy storage systems without requiring large line frequency transformers.

After the converter structure and control system description, a parameter sensitivity analysis and stability studies have been performed pointing out that the influence of the variation of the ratio between the supply and the converter filter inductances on stability, dc-link voltage, and current tracking is negligible on real cases.

The effectiveness of the proposed control strategy in a natural reference frame is verified through different study cases including faulty operating conditions. The analysis has been performed at first in a Matlab/Simulink environment using a model of the converter suitable for both average and switching simulations. The simulation results have shown that the control system can track active and reactive power demands under different power reference profiles and grid operating conditions; moreover, the control system presents a fast and accurate current tracking. A good decoupling of the active and reactive power control is obtained in all considered cases. The supply currents are essentially sinusoidal even under unbalanced supply voltage conditions. The average dc-link voltage presents only small deviations from the rated value; in normal operating conditions the maximum dc voltage ripple reaches a value of about 1.5%. The predictive controller can also reject significantly the harmonic distortion in the supply voltage without using, unlike other control strategies, any additional filter in the control loop which can present critical issues on parameters tuning and stability. Moreover, the currents are individually controlled on each phase adding more flexibility to the UNIFLEX-PM.

Finally, experimental tests on a 300 kVA prototype have successfully validated the simulation conclusions demonstrating

the capability of the proposed power conversion system for electricity routing and power flow control in future power grids.

APPENDIX

See Table III for a list of European and International grid standards for DG connection.

ACKNOWLEDGMENT

The authors would like to acknowledge the contributions to this project by all partners of the UNIFLEX-PM consortium: University of Nottingham, Aalborg University, Ecole Polytechnique Federale de Lausanne, Università degli Studi di Genova, ABB Secheron, Dynex Semiconductor LTD, Areva T&D, European Power Electronics Association (EPE).

REFERENCES

[1] New ERA for Electricity in Europe. Distributed Generation: Key Issues, Challenges and Proposed Solutions European Commission, EUR 20901, 2003, ISBN 92-894-6262-0.

[2] Towards Smart Power Networks. Lessons Learned from European Research FP5 Projects 2005, European Commission, EUR 21970, ISBN 92-79-00554-5.

[3] F. Iov, F. Blaabjerg, R. Bassett, J. Clare, A. Rufer, S. Savio, P. Biller, P. Taylor, and B. Sneyers, "Advanced power converter for universal and flexible power management in future electricity network," presented at the CIRED, Vienna, Austria, May 2007.

[4] B. Wu, *High-Power Converters and AC Drives*. New York: IEEE Press—Wiley Interscience, 2006.

[5] V. G. Agelidis, G. D. Demetriades, and N. Flourentzou, "Recent advances in high-voltage direct-current power transmission systems," in *Proc. IEEE Int. Conf. Ind. Technol. (ICIT)*, Dec. 2006, pp. 206–213.

[6] A. Rufer, "Today's and tomorrow's meaning of power electronics within the grid interconnection," presented at the 12th Eur. Conf. Power Electron. (EPE), Aalborg, Denmark, Sep. 2007, keynote paper.

[7] F. Blaabjerg and F. Iov, "Wind power—A power source now enabled by power electronics," presented at the 9th Brazilian Power Electron. Conf. (COBEP), Blumenau, Santa Catarina, Brazil, Oct. 2007.

[8] Y. H. Liu, J. Arrillaga, and N. R. Watson, "Cascaded H-bridge voltage reinjection—Part II: Application to HVDC transmission," *IEEE Trans. Power Del.*, vol. 23, no. 2, pp. 1200–1206, Apr. 2008.

[9] D. Soto and T. C. Green, "Voltage balance and control in a multi-level unified power flow controller," *IEEE Trans. Power Del.*, vol. 16, no. 4, pp. 732–738, Oct. 2001.

[10] B. R. Lin and T. C. Wei, "A novel NPC inverter for harmonics elimination and reactive power compensation," *IEEE Trans. Power Del.*, vol. 19, no. 3, pp. 1449–1456, Jul. 2004.

[11] A. Bellini, S. Bifaretti, and S. Costantini, "Implementation on a microcontroller of a space vector modulation technique for NPC inverters," in *Proc. IEEE Int. Symp. Ind. Electron. (ISIE)*, May 2004, pp. 935–940.

[12] Y. Li and B. Wu, "A novel DC voltage detection technique in the CHB inverter-based STATCOM," *IEEE Trans. Power Del.*, vol. 23, no. 3, pp. 1613–1619, Jul. 2008.

[13] D. Soto and T. C. Green, "A comparison of high-power converter topologies for the implementation of FACTS controllers," *IEEE Trans. Ind. Electron.*, vol. 49, no. 5, pp. 1072–1080, Oct. 2002.

[14] Y. Cheng, C. Qian, M. L. Crow, S. Pekarek, and S. Atcitty, "A comparison of diode-clamped and cascaded multilevel converters for STATCOM with energy storage," *IEEE Trans. Ind. Electron.*, vol. 53, no. 5, pp. 1512–1521, Oct. 2006.

[15] A. Nabae, I. Takahashi, and H. Akagi, "A new neutral-point-clamped PWM-inverter," *IEEE Trans. Ind. Appl.*, vol. IA-17, no. 5, pp. 518–523, 1981.

[16] M. Marchesoni and M. Mazzucchelli, "Multilevel converters for high power ac drives: A review," in *Proc. IEEE Int. Symp. Ind. Electron.*, 1993, pp. 38–43.

[17] D. Gerry, P. Wheeler, J. Clare, R. J. Bassett, C. D. M. Oates, and R. W. Crookes, "Multi-level, multi-celular structures for high voltage power conversion," presented at the EPE, Graz, Austria, Aug. 2001.

[18] M. C. Magro and S. Savio, "Dependability and impact analysis for a universal and flexible power management system," *EPE J.*, vol. 19, no. 4, pp. 51–58, Dec. 2009.

[19] P. Rodriguez, J. Pou, J. Bergas, J. I. Candela, R. P. Burgos, and D. Boroyevich, "Decoupled double synchronous reference frame PLL for power converters control power electronics," *IEEE Trans. Power Electron.*, vol. 22, no. 2, pp. 584–592, Mar. 2007.

[20] R. Teodorescu and F. Blaabjerg, "Flexible control of small wind turbines with grid failure detection operating in stand-alone or grid-connected mode," *IEEE Trans. Power Electron.*, vol. 19, no. 5, pp. 1323–1332, Sep. 2004.

[21] R. Teodorescu, F. Iov, and F. Blaabjerg, "Flexible development and test system for 11 kW wind turbine," in *Proc. IEEE PESC*, Jun. 2003, vol. 1, pp. 67–72.

[22] S. Bifaretti, P. Zanchetta, Y. Fan, F. Iov, and J. Clare, "Power flow control through a multi-level H-bridge based power converter for universal and flexible power management in future electrical grids," in *Proc. 13th Int. Conf. Power Electron. Motion Control Conf. (EPE-PEMC)*, Sep. 2008, pp. 1771–1778.

[23] W. Lenwari, M. Sumner, P. Zanchetta, and M. Culea, "A high performance harmonic current control for shunt active filters based on resonant compensators," in *Proc. IECON*, Nov. 2006, pp. 2109–2114.

[24] M. Ciobotaru, F. Iov, P. Zanchetta, Y. De Novaes, and J. Clare, "A stationary reference frame current control for a multi-level H-bridge power converter for universal and flexible power management in future electricity network," in *Proc. Power Electron. Specialists Conf. (PESC)*, Jun. 2008, pp. 3943–3949.

[25] A. Bellini, S. Bifaretti, and S. Costantini, "A hysteresis modulation technique for NPC inverter in digitally controlled induction motor drives," presented at the 10th Int. Conf Power Electron. Motion Control (EPE-PEMC), Dubrovnik, Croatia, Sep. 2002.

[26] J. Rodriguez, J. Pontt, C. A. Silva, P. Correa, P. Lezana, P. Cortes, and U. Ammann, "Predictive current control of a voltage source inverter," *IEEE Trans. Ind. Electron.*, vol. 54, no. 1, pp. 495–503, Feb. 2007.

[27] P. Zanchetta, D. B. Gerry, V. G. Monopoli, J. C. Clare, and P. W. Wheeler, "Predictive current control for multilevel active rectifiers with reduced switching frequency," *IEEE Trans. Ind. Electron.*, vol. 55, no. 1, pp. 163–172, Jan. 2008.

[28] S. Bifaretti, P. Zanchetta, M. Ciobotaru, F. Iov, and J. C. Clare, "Power flow control through the UNIFLEX-PM under different network conditions," *EPE J.*, vol. 19, no. 4, pp. 32–41, Dec. 2009.

[29] M. Ciobotaru, F. Iov, P. Zanchetta, Y. De Novaes, and F. Blaabjerg, "Study and analysis of a natural reference frame current controller for a multi-level H-bridge power converter," in *Proc. Power Electron. Specialists Conf. (PESC)*, Jun. 2008, pp. 2914–2920.

[30] A. Bellini, S. Bifaretti, and V. Iacovone, "Robust PLL algorithm for three-phase grid-connected converters," *EPE J.*, vol. 20, no. 4, Dec. 2010.

[31] S. Bifaretti, P. Zanchetta, A. Watson, L. Tarisciotti, A. Bellini, and J. Clare, "A modulation technique for high power AC/DC multilevel converters for power system integration," presented at the IEEE Energy Conv. Congr. Expo. (ECCE), Atlanta, GA, Sep. 2010.

[32] "Grid connection of wind turbines to networks with voltages below 100 kV," EnergiNet Tech. Reg. TF 3.2.6, p. 29, May 2004.

[33] "Grid connection of wind turbines to networks with voltages above 100 kV," EnergiNet Tech. Reg. TF 3.2.5, p. 25, Dec. 2004.

Stefano Bifaretti (M'07) was born in Rome, Italy, in 1974. He received the Laurea degree and the Ph.D. degree in electronic engineering from University of Rome Tor Vergata, Italy, in 1999 and 2003, respectively.

Since 2004, he has been an Assistant Professor at Department of Electronic Engineering of the University of Rome Tor Vergata, where he is a Lecturer in power electronics. In 2007 he was with the PEMC research group at the University of Nottingham, U.K., collaborating with the UNIFLEX-PM European project. He has published over 60 papers in international journals and conferences. His research interests include power electronics converters, industrial drives, and photovoltaic conversion systems.

Pericle Zanchetta (M'00) received the five-year Laurea degree in electronic engineering and the Ph.D. degree in electrical engineering from the Technical University of Bari, Italy, in 1993 and 1997, respectively.

In 1998 he became Assistant Professor of Power Electronics at the Technical University of Bari. In 2001 he became a Lecturer in the PEMC research group at the University of Nottingham, U.K., where he is currently Associate Professor in control of power electronics systems. He has published over 130 papers in international journals and conferences. His main research interests are in the field of power quality and harmonics, active power filters, power systems impedance estimation, advanced control of power converters, control design, and system identification using genetic algorithms.

Alan Watson (S'03–M'07) received the M.S. and Ph.D. degrees in electronic engineering and electrical and electronic engineering from the University of Nottingham, U.K., in 2004 and 2008, respectively.

He is currently a Research Fellow in the Power Electronics, Machines and Control Group at the University of Nottingham. His research interests include multilevel converters, advanced modulation schemes, and power converter control.

Dr. Watson is a Member of the Institution of Engineering and Technology (IET).

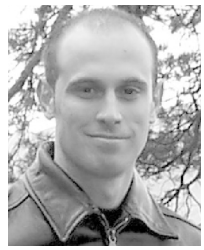

Luca Tarisciotti received the M.S. degree in electronic engineering from the University of Rome Tor Vergata, Italy, in 2009. He is currently working toward the Ph.D. degree in electrical and electronic engineering at the University of Nottingham, U.K.

His research interests include multilevel converters, advanced modulation techniques, and power converter control.

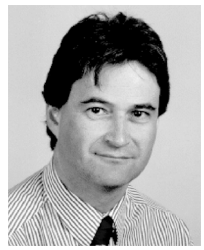

Jon C. Clare (M'90–SM'04) was born in Bristol, U.K. He received the B.Sc. and Ph.D. degrees in electrical engineering from the University of Bristol, U.K.

From 1984 to 1990, he was a Research Assistant and Lecturer at the University of Bristol involved in teaching and research in power electronic systems. Since 1990 he has been with the Power Electronics, Machines and Control Group at the University of Nottingham, U.K., and is currently Professor in Power Electronics and Head of Research Group. His research interests are power electronic converters and modulation strategies, variable speed drive systems, and electromagnetic compatibility.